Evaluation of the accuracy of the Structure from Motion technique applied to Photogrammetric Mapping of Corridors

https://doi.org/10.56238/levv15n39-036

Natalia Carvalho de Amorim[1], Edson Appeared Mitishita[2].

ABSTRACT

The advantages offered by the use of RPA technology combined with the algorithms implemented by the SfM technique and its variants have made Photogrammetry supported by RPA and SfM an economical, fast and widely used solution in various branches of Engineering. Despite many studies on the accuracy achieved in digital cartographic products generated through these technologies, little is discussed about the case of corridors. In this context, the objective of this work is to investigate the positional accuracy achieved in the mapping of a 1.3 km long corridor through the adoption of different amounts of control points and different amounts of lanes. Accuracy assessment was performed based on the Mean Square Error (NDE) values of the checkpoints and trend analysis. The experiments showed that the adoption of control points positioned every five and ten photogrammetric bases can achieve accuracy between 2-2.6 GSD and eliminate planimetric and altimetric statistical trends in the RMSE values of the checkpoints that adopt two or three bands. In addition, the experiments performed showed that increasing the number of bands does not necessarily imply a decrease in the NDE values of checkpoint discrepancies.

Keywords: Photogrammetry, Corridor, Adjustment, SfM.

[1] Master in Geodetic Sciences
Federal University of Paraná
[2] Doctor in Geodetic Sciences
Federal University of Paraná

INTRODUCTION

The technological advancement experienced in recent years has brought new approaches and paradigm shifts to Geodetic Sciences. Technologies such as Unmanned Aerial Vehicles (UAVs) and algorithms for detecting and describing notable points in digital images have shown high impact in the context of analysis and extraction of geospatial information through autonomous methods.

The UAV models found on the market are the most diverse, and designed to meet the different existing demands, and, for this reason, it is difficult to attribute a single concept to this equipment (Hardin, Jensen, 2011). In Brazil, the National Civil Aviation Agency (ANAC), which regulates the use of UAVs by civilians, has established two classes to conceptualize this equipment: The Aero model, which are all types of UAVs used for recreational purposes; and Remotely Piloted Aircraft (RPAs), which comprise UAVs piloted through a remote control station and used for non-recreational activities. In this work, the term RPA is used to refer to this equipment, popularly known as drones.

The RPA models commonly used for photogrammetric applications are: RPA-SPS (Standard Positioning Service), which provides the positioning solution based on the open signals of the GNSS System; RPA-RTK (Real-Time Kinematic), which are models that have an RTK System and allow the correction of systematic positioning errors in real time (Sopchaki et al, 2018) and RPA-PPK (Post-Processing Kinematic), models that have a system that allows the post-processing of RPA positions at the time of image acquisition. This equipment quickly became popular in the professional and scientific environment for offering advantages such as the low investment required for its acquisition and operation, especially in the case of SPS models, the agility in the acquisition of digital aerial images and the high precision and accuracy achieved with the use of RTK and PPK systems.

On the other hand, the growing advancement achieved in the areas of Computer Vision, Digital Image Processing and Hardware has strongly contributed to the adoption of new approaches by conventional Photogrammetry, the main one being the Structure from Motion technique, currently available in several specialized software (Javernick, Brasington and Caruso, 2014).

Structure from Motion (SfM) refers to the problem of determining the three-dimensional position of a set of points observed in a set of images when there is only a sparse set of correspondences between these points in the images obtained by a moving sensor (Szeliski, 2010, p. 345). A parallel can be established between Computer Vision and Photogrammetry since these sciences have the same goal in common: To recover the three-dimensional geometry of a surface through a set of images obtained from different points of view (moving sensor). Thus, it can be said that the SfM technique works based on the principles of stereogrammetric photogrammetry (Westoby et al, 2012).

The growing demand for process automation has led to the rapid adoption of Photogrammetry supported by RPA and SfM by the professional and scientific communities, using these technologies to generate digital cartographic products in an automated way, making the planning and decision-making process less costly and more agile.

Thus, several studies on the positional quality achieved by the use of Photogrammetry supported by RPA and SfM have been carried out in the last five years: Rehak and Skaloud (2015) presented a study that verified the positional quality achieved in the mapping of a corridor and an image block and concluded that to achieve an accuracy between 3 cm and 5 cm, the position and attitude of the camera at the time of taking must be known with high accuracy; James et al (2017) conducted a study on the accuracy achieved in the generation of digital elevation models, testing different configurations of control points on the ground and the use of different parameters available in the specialized software used in the study; Meinen and Robinson (2020) present a comparative study between UAV-supported Digital Photogrammetry and Traditional Photogrammetry in the application of river slope mapping. The study revealed that, in the analyzed scenario, Photogrammetry supported by RPA and SfM presented lower values of mean squared error at the checkpoints; Elkhrachy (2021) experimented with four different distributions of ground control points and two different photogrammetric software with the goal of producing accurate 3D geospatial information. The model obtained in the study presented by Elkhrachy achieved RMSE values in the range of 4-6 cm and 5-6 cm, for horizontal and vertical coordinates of the checkpoints, respectively.

Despite the diversity of studies carried out to verify the accuracy achieved in photogrammetric surveys using RPA and SfM, few studies have analyzed the specific case of corridor mapping. Cases such as mapping transmission lines, railways, and rivers are some examples of photogrammetric applications that configure the geometry of a corridor. It is worth mentioning that, due to their geometric configuration, corridors tend to have analytical deficiencies that can cause a decrease in the precision achieved in this type of mapping.

In this context, this study aims to investigate the accuracy achieved in the mapping of a corridor using an RPA for image acquisition and the Metashape software, which implements a variant of the Structure from Motion technique. The evaluation is carried out through the use of checkpoints positioned along the photogrammetric block, in this way, this work evaluates the quality of the adjustment of the parameters through the root of the estimated mean squared error for the coordinates of the checkpoints and how the arrangement of these points influences this quality.

MATERIAL AND METHODS

STUDY AREA AND AERIAL PHOTOGRAMMETRIC SURVEY

The study area is located within the Polytechnic Campus of the Federal University of Paraná, in the State of Paraná, Brazil. Figure 1 shows the corridor that extends for approximately 1.3 km within the campus area.

The image acquisition process was carried out using the RPA Phantom 4 Pro, equipment that has a camera with a 1-inch CMOS sensor, generating images of 4864 x 3648 pixels, which results in a geometric pixel resolution of approximately 2.61 micrometers. The equipment also has a GNSS sensor that records observations of the position of the center of perspective with planimetric accuracy of 1.5 m and altimetric accuracy of 0.5 m, according to technical specifications provided by the manufacturer. The flight was performed at a height of approximately 100 m and the lateral and longitudinal overlap rates were 60% and 80%, respectively. High values of overlap between bands were adopted to increase the redundancy of observations of connection points between images and between bands.

Figure 1 – Flight Plan

Through the adopted flight configuration, a GSD of approximately 3.0 cm was obtained, which allows the observation of photoidentifiable features, such as crosswalk corners, traffic signaling lanes, manhole covers, among others.

DATA PROCESSING

Data processing was performed by testing different spatial distributions of control points and different aerial photogrammetric coverings. The experiments were carried out using one, two and three bands. For each number of lanes, the control point configurations of fifteen, ten and five photogrammetric bases were tested. For all tests, the camera's interior orientation parameters were estimated through self-calibration during the adjustment of the photogrammetric corridor, adopting the Conrady-Brown model, therefore, in these experiments, focal length (f), coordinates of the main point (cx, cy), symmetrical radial distortion coefficients (K1, K2, K3) and off-center distortion coefficients (P1, P2, P3) are considered for corridor adjustment. The images were processed using the Metashape software. Figure 2 schematically presents the methodology used for the processing of the images. Each step will be described in detail in the following subsections.

Figure 2 – Flowchart of the Meotodology adopted

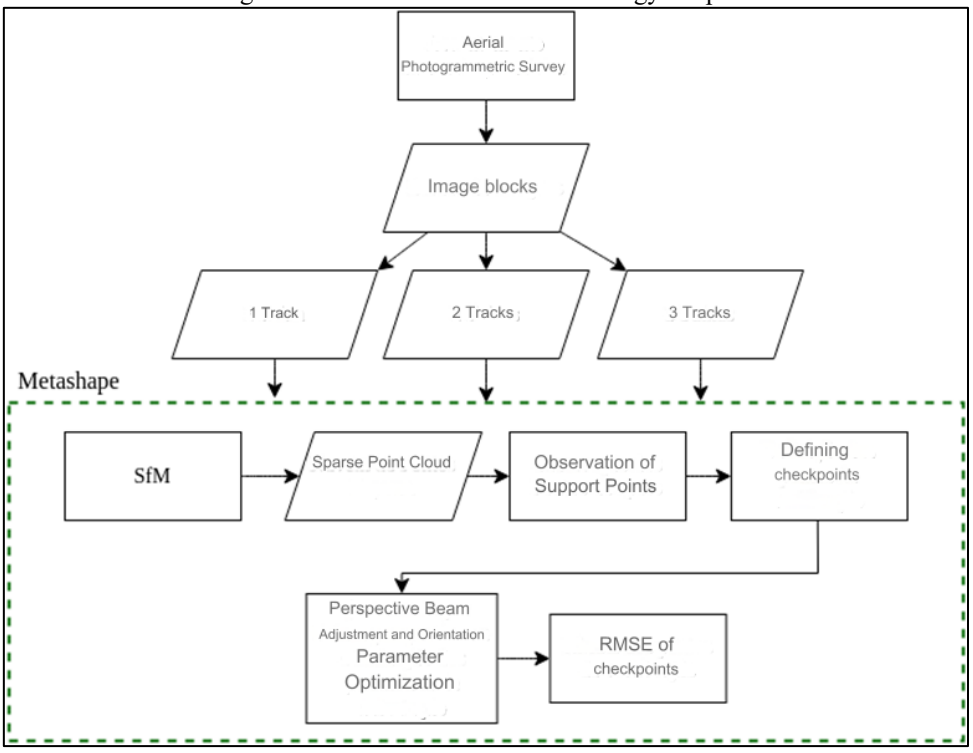

DISTRIBUTION OF CONTROL POINTS

To improve the accuracy achieved in the adjustment of the photogrammetric block, the use of control points is employed. The planialtimetric coordinates of the control and verification points were extracted from the orthomosaic made available in the cartographic database maintained by the

UFPR Campus Map project. The orthomosaic has a spatial resolution of 5 cm, with total planimetric error values of 6 cm, and the MDE has a total altimetric error of 4 cm \cite{delazari2019ufpr}. Thus, for each number of tracks, three control point configurations were tested:

- A pair of control points are inserted every fifteen aerial photogrammetric bases;
- A pair of control points are inserted every ten aerial photogrammetric bases;
- A pair of control points are inserted every five aerial photogrammetric bases.

For further clarification on the distribution of control points used, Figure 3 presents the geometric definition of the aerial photogrammetric base, represented by the letter B, the photobase (b), the width of the photograph in the object space (D), as well as the width of the photograph in the image space (d). The Air Photogrammetric Base, also known as the Air Base, is the distance between two positions of the camera's perspective center at the time of taking the photograph and plays an important role in photogrammetric mapping. For this reason, the number of aerial photogrammetric bases is adopted as the standard to describe the distribution of control points.

Figure 3 – Aerophotogrammetric Base

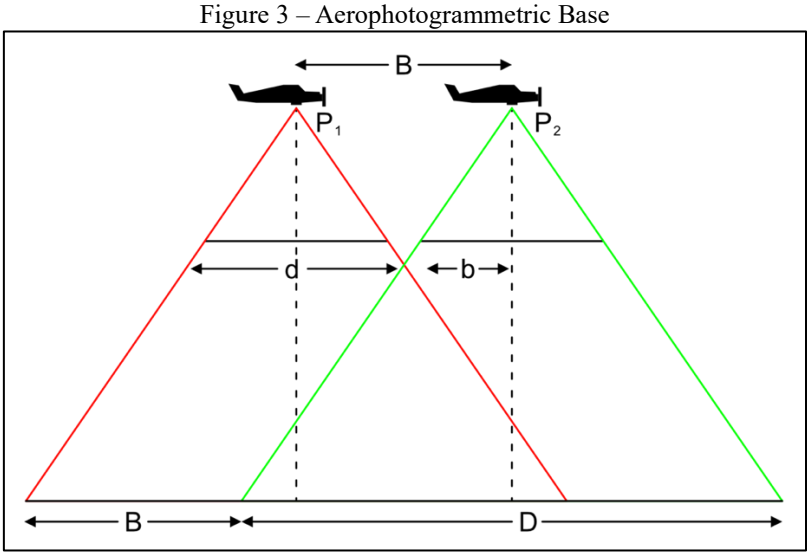

Figures 4 and 5 show the distribution of the control and verification points adopted in each of the experiments carried out. The control and verification points are presented in red and blue, respectively.

Figure 4 – Distribution of Control and Verification Points for one-lane experiments

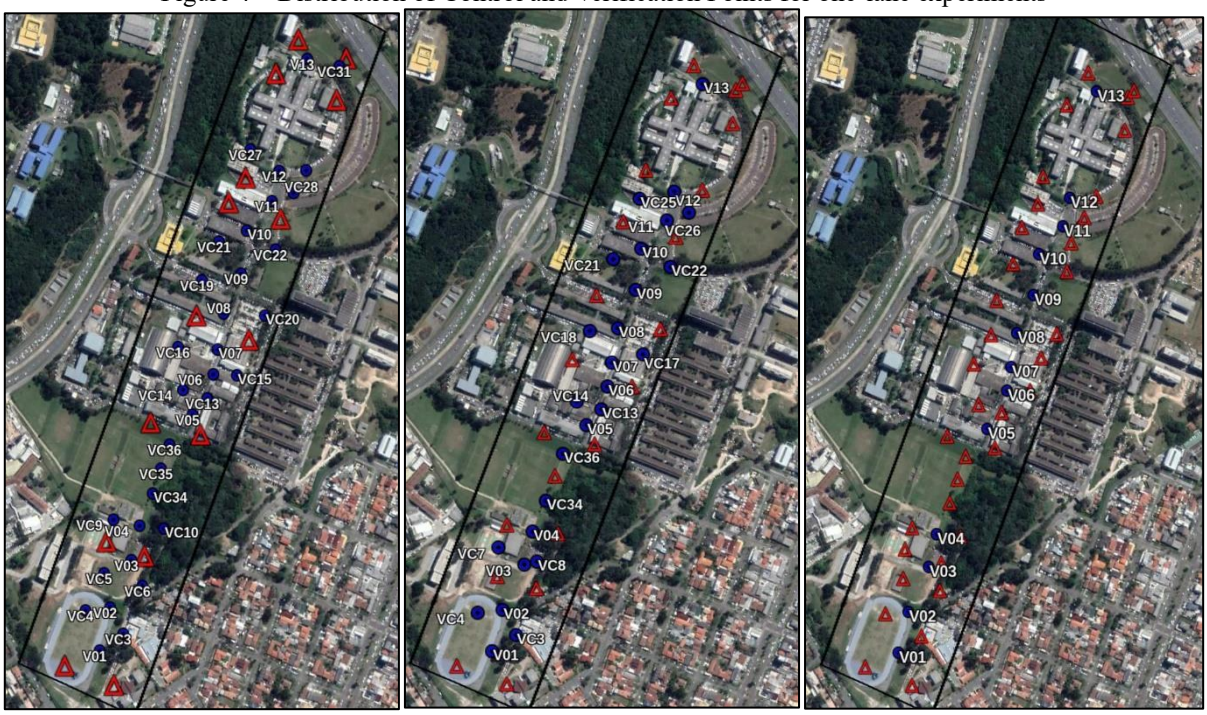

Figure 4 shows the spatial distribution of the control and verification points used in the experiments using a single photogrammetric strip. In Figure 3 (a) the control points are placed every fifteen photogrammetric bases, resulting in the use of fifteen control points; Subsequently, the control points are placed every ten photogrammetric bases, as shown in Figure 3 (b), resulting in the use of twenty-one control points and, finally, the number of control points is increased again, and the control points are placed every five photogrammetric bases, resulting in the maximum number of control points used in this set of experiments, that is, thirty-four control points.

Figure 5 – Distribution of Control and Verification Points for two-lane experiments

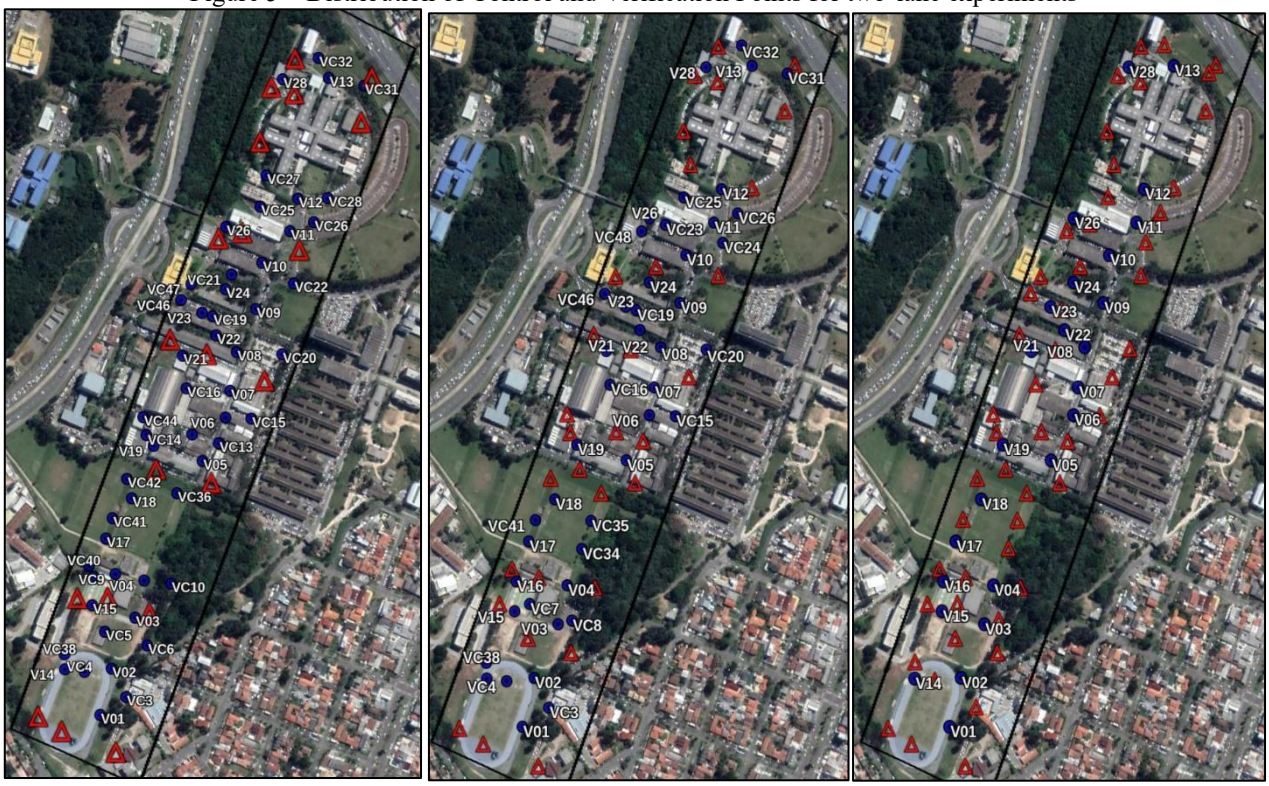

Figure 5 shows the spatial distribution of the control and verification points used to carry out the experiments using image blocks with two and three strips. In Figure 4(a), 4(b) and 4(c), the control points are placed every fifteen, ten and five photogrammetric bases, respectively. The same distribution of control points is used in the cases of two and three bands due to the restrictive nature of the study area, which made it impossible to observe new control points due to obstructions.

The three different image coatings were experimented to verify if the addition of stripes can make the number of control points used more flexible, maintaining the same precision achieved in the experiment using five photogrammetric bases.

ANALYSIS OF POSITIONAL ACCURACY

Accuracy was assessed by adopting the mean square error (NDE) values of checkpoint discrepancies as a metric. The expected accuracies were defined as established by Kraus (2011), in the Normal Case of Photogrammetry. For this condition, the accuracies (planimetric and altimetric) of the adjustment of the photogrammetric block can be estimated as a function of the scale of the photographs and the ratio between the air base and the flight height. Thus, the control point planimetric discrepancy NDE is expected to have a maximum value of 8.6 cm and 15 cm for the control point altimetric discrepancy NDE.

Additionally, a trend analysis was performed to verify the presence of systematic errors in the planialtimetric coordinates of the checkpoints. This analysis was done through the statistical hypothesis test where the hypotheses tested were:

$$H_0: \mu = 0$$
$$H_1: \mu \neq 0$$

The hypothesis test was conducted as suggested by Galo and Camargo (1994), where M is the population mean, H_0 and H_1 are the null and alternative hypotheses, respectively. To validate one of the hypotheses, Student's t-test was performed.

If the average of the checkpoint discrepancies is statistically equal to zero, there is no trend in these discrepancies. By comparing a calculated value of t with its tabulated value, the null hypothesis may or may not be discarded. Thus, the calculated value is obtained from Equation 2.

$$t_{calc} = \frac{\Delta}{S^2}\sqrt{n}$$

Where:

- Δ is the average sample value of the discrepancies of a coordinate of the checkpoints;
- *S2* is the sample variance of the discrepancies of a coordinate of the checkpoints;
- *n is the sample size.*

The calculated value of t is compared to the tabulated value with a significance level of 90% and the alternative hypothesis is discarded if the condition demonstrated in Equation 4 is true.

$$|t_{calc}| < t_{n-1,\alpha/2}$$

If the condition of Equation 3 is not satisfied, the null hypothesis is discarded, and the existence of a trend in the discrepancies of the checkpoints can be assumed.

RESULTS AND DISCUSSION

Figure 6 shows the mean squared error (NDE) values calculated for the planimetric and altimetric discrepancies of the checkpoints in the photogrammetric coating experiments with one (Fig. 5 a), two (Fig. 5 b) and three stripes (Fig. 5 c). Each figure shows the planimetric and altimetric mean square error for the three different control point distributions (fifteen, ten, and five photogrammetric bases).

Figure 6(a) shows that when the number of control points is increased, the NDE values decrease. The lowest NDE values are observed in the case of control points placed every five photogrammetric bases, which presented values of 6.019 cm for planimetric discrepancies and 5.69 cm for altimetric discrepancies, these values satisfy the tolerance established for this experiment. The expected altimetric accuracy (15 cm) was achieved in all three distributions experimented in the case of single-lane corridor mapping, but the lowest NDE values were achieved in the case of control points inserted every five airbases.

Figure 6 – Checkpoint Discrepancies NDE

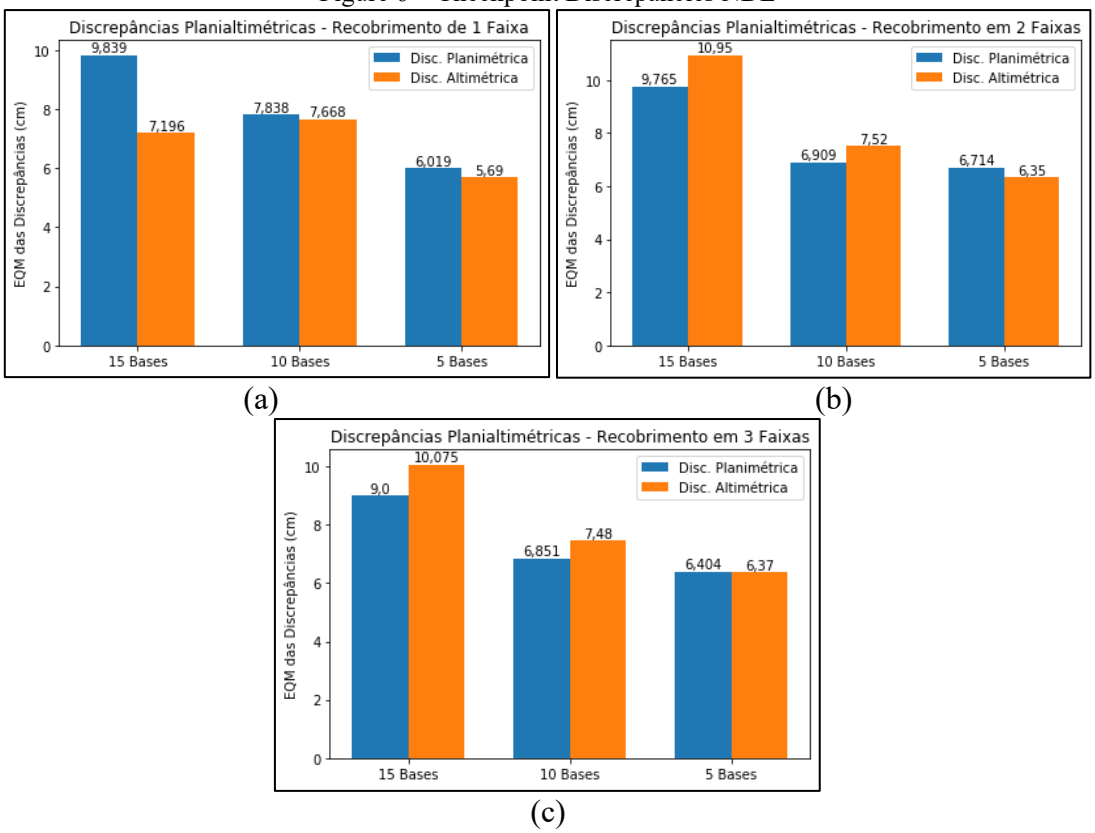

Looking now at Figure 6 b, it can be seen that the planimetric mean square error obtained in the experiment using control points every fifteen bases does not meet the expected precision established in this study (8.6 cm), being 3.754 cm greater than the NDE presented in Figure 6 a (15 bases). This increase happens because the increase in the number of photographs when there is a deficient distribution of control points creates fragile areas and systematic errors are propagated to the coordinates of the control points located in these regions. Thus, there is evidence that the addition of lanes does not necessarily allow the flexibility of the number of control points adopted, but requires a replanning of these. When the number of control points used increases, that is, adopting the distribution of ten and five bases, it can be observed that the NDE planimetric and altimetric discrepancies have their values reduced.

Still observing the NDE values presented in Figure 5 b and comparing them with the values presented in Fig. 6 a, it can be seen that the addition of the second band did not cause a significant reduction in planimetric and altimetric NDE values in the case of control points distributed in every five air bases (less than 1 cm), however a significant reduction in the NDE of planimetric discrepancies could be observed in the case of experiments with positioned control points for every ten bases, which in the case of the covering with a stripe have values of 7.838 cm (Fig. 5 a) and 6.909 cm (Fig 5b), representing almost 1 cm of decrement with the addition of the second stripe and an intensified distribution of control points.

The NDE values of the checkpoint discrepancies shown in Figure 5c, obtained in the three-band coating experiment, are similar to those shown in the case of two bands (Fig. 5b). For all control point distributions tested with two and three ranges, the difference between the planimetric and altimetric NDE values is less than 0.5 cm. Thus, we can conclude that the addition of the third band did not cause a significant reduction in the planimetric or altimetric mean square error. In the different distributions of control points and number of strips tested, only the distribution of the fifteen photogrammetric bases did not satisfy the tolerance established in this work.

For further clarification of the values presented in Figure 5, an analysis of statistical trends in the experiments was also performed. Table 1 summarizes this analysis by categorizing the results into four distinct types: 1) Unbiased means that the three coordinate components (X, Y, and Z) are free of bias; 2) Planimetric Trend means that at least one or both of the planimetric coordinates (X, Y) are biased and 3) Altimetry Trend means that only the Z coordinate is biased, and 4) Trend means that all components of the coordinates (X, Y, and Z) are biased.

Table 1 - Trend Analysis

	5 Bases	10 Bases	15 Bases
One track	Non-biased	Planimetric Trend	Altimetry Tendency
Two Tracks	Planimetric Trend	Non-biased	Biased
Three Tracks	Planimetric Trend	Non-biased	Biased

Tables 2 to 4 present the statistical metrics obtained in the trend analysis, as well as the detailed classification for each axis.

Table 2 - Trends in checkpoint discrepancies - Photogrammetric coverage with a stripe

Fifteen bases			
	X (cm)	Y (cm)	Z (cm)
Average	0,209	2,03	3,868
t calc.	0,1969	1,5643	3,6628
$T_{(33,\ 10/2)}$	1,6924		
Biased	No	No	Yes
Ten Bases			
	X	And	With
Average	2,099	1,672	1,572
t calc.	1,9508	1,7377	1,0681

$t_{(26, 10/2)}$	1,7056		
Biased	Yes	Yes	No
Five Bases			
	X	And	With
Average	-0,483	0,035	2,428
t calc.	-0,5817	0,0234	1,6361
$t_{(12, 10/2)}$	1,7823		
Biased	No	No	No

Table 3 - Trends in checkpoint discrepancies - Photogrammetric coverage with two stripes

Fifteen bases			
	X (cm)	Y (cm)	Z (cm)
Average	1,647	1,716	4,022
t calc.	1,7515	1,9883	2,9283
$t_{(55, 10/2)}$	1,637		
Biased	Yes	Yes	Yes
Ten Bases			
	X	And	With
Average	-0,898	0,5727	-0,463
t calc.	-1,25	0,77	-0,4095
$t_{(44, 10/2)}$	1,6794		
Biased	No	No	No
Five Bases			
	X	And	With
Average	1,7654	0,4168	-0,7061
t calc	1,8826	0,4492	-0,5481
$t_{(24, 10/2)}$	1,7109		
Biased	Yes	No	No

Looking at Table 2, it can be seen that, when the aerial coverage of a single lane is adopted, only the distribution of control points every five bases is sufficient to completely eliminate the trends in the discrepancies of the checkpoints. It is also noted that when the distribution of ten bases is adopted, planimetric trends appear in the discrepancies of the checkpoints. This may occur due to the difficulty of breaking the existing correlations between the parameters involved in the adjustment of the photogrammetric corridor using only one strip.

Table 3 shows the results of the statistical analysis of trends for the experiments of photogrammetric coverage of the corridor with two strips. In this case, the distribution of support points inserted in every ten bases was sufficient to eliminate planimetric and altimetric trends, while in the case of fifteen bases, all components were biased. The experiment of inserting control points every five bases showed a planimetric trend in component X, indicating that the decrease in degrees of freedom, caused by the adoption of many control points, was not the best alternative for the reduction of systematic errors present in the adjustment.

Table 4 presents the statistical metrics for trend analysis regarding the photogrammetric coverage experiments of the corridor with three strips. A behavior similar to the previous experiment (Table 3) is observed when comparing the experiments of control points inserted every ten and five bases, since the mean of the discrepancies of the checkpoints presents a millimetric difference between these two cases. This analysis shows that the addition of a strip, without modifying the

distribution of control points, does not imply the elimination of planialtimetric trends, and the distribution of control points adopted is more critical for the distribution of the systematic errors involved.

Table 4 - Trends in checkpoint discrepancies - Photogrammetric coverage with three stripes

Fifteen bases			
	X (cm)	Y (cm)	Z (cm)
Average	1,314	1,727	4,015
t calc.	1,5403	2,1252	3,2231
$t_{(55, 10/2)}$	1,673		
Biased	No	Yes	Yes
Ten Bases			
	X	And	With
Average	-0,866	0,593	-0,373
t calc.	-1,1974	0,8152	-0,3326
$t_{(44, 10/2)}$	1,6794		
Biased	No	No	No
Five Bases			
	X	And	Z
Average	1,665	0,052	-0,771
t calc.	1,9174	0,5775	0,598
$t_{(24, 10/2)}$	1,7109		
Biased	Yes	No	No

The results obtained in the experiments carried out, in terms of planimetric and altimetric NDEs, are in line with those presented by Ferrer-González et al (2020), who showed in their work that increasing the number of control points improves the accuracy achieved in the adjustment of the photogrammetric corridor. The authors also showed that vertical NDE values are higher than planimetric NDE values, however, this research also performed an analysis of the influence of the number of lanes on corridor mapping, noting that the number of control points employed in the adjustment is more critical to reduce vertical and horizontal NDE values than the addition of bands.

In terms of GSD, this work achieved planimetric and altimetric accuracies between 2 GSD and 2.6 GSD through the distribution of control points of five and ten photogrammetric bases. Comparing the precision achieved in this study with the precision achieved in the work presented by Skarlatos et al (2013), it can be noted that the experiments presented here achieved better precision, since the vertical and horizontal accuracies presented in their study were more than three times the value of the GSD. Comparing the accuracy achieved, still in terms of GSD, with the precision achieved presented by Elkhrachy (2021), two and three times GSD for horizontal and vertical accuracy, respectively, we can observe that the present study achieved similar accuracy since it presented RMSE of 2-2.6 times GSD using control point distribution of five and ten photogrammetric bases.

FINAL CONSIDERATIONS

This study aimed to evaluate the accuracy achieved by the adjustment performed through the Structure from Motion technique applied to the geometry of a corridor, analyzing how the number of control points and the number of photogrammetric ranges influence the EQM values of the checkpoints. A trend analysis of checkpoint discrepancies was also performed.

The experiments carried out showed that the number and distribution of the control points adopted exert a greater influence on the NDE values, while the number of bands can contribute to the elimination of trends in planimetric and altimetric discrepancies. Thus, when working with corridor surveying through the SfM BBA, it is recommended to adopt at least two bands, placing a set of control points at most every ten ground bases to decrease the EQM value of the checkpoints, as well as to avoid planimetric and altimetric trends.

In this study, the expected values for NDE of the checkpoints were 8.6 cm and 15 cm for planimetric and altimetric components, respectively, and it is noteworthy that the altimetry values of NDEs observed in all experiments agreed with the expected values defined in this work. Since it is a difficult task to obtain NDE altimetric values lower than planimetric ones, we can again attest to the advantage of using the control point distribution every ten ground bases, since the planimetric and altimetric NDE values were similar, free of trends and reached an accuracy of 2 to 2.6 GSD.

Regarding the number of lanes used in the experiments, no significant difference was observed between the NDE values considering the same control point distributions and varying the number of lanes used in the corridor mapping. Thus, it can be concluded that the control point distribution adopted is more crucial than the number of bands to reduce the NDE values of the checkpoints, however, the use of more bands can completely eliminate the trends in the discrepancies of the checkpoints.

Through the experiments carried out and the results presented, we can perceive the advantages of using UAV and Digital Photogrammetry techniques as Bundle Block Adjustment supported by the SfM technique. In addition to providing cost and time reduction in photogrammetric surveying, these modern approaches allow to achieve high precision values depending on the specifications and strategies of the project.

It is suggested for future works to carry out experiments applying SfM BBA in corridors, studying the influence of the addition of oblique photographs, the influence of pre-calibration and the precision achieved through the Integrated Sensor Orientation technique.

ACKNOWLEDGMENTS

The authors thank the National Council for Scientific and Technological Development (CNPq) for granting the scholarship, and the Federal University of Paraná (UFPR) for providing the necessary infrastructure to conduct the research.

REFERENCES

ANAC. (2017). Regulamento Brasileiro da Aviação Civil Especial. Available at: https://www.anac.gov.br/assuntos/legislacao/legislacao-1/rbha-e-rbac/rbac/rbac-e-94/@@display-file/arquivo_norma/RBACE94EMD00.pdf.

Delazari, L. S., Filho, L. E., & Skroch, A. L. S. D. (2019). UFPR CampusMap: A laboratory for Smart City developments. AbICA, 1, 57.

Elkhrachy, I. (2021). Accuracy assessment of low-cost unmanned aerial vehicle (UAV) photogrammetry. Alexandria Engineering Journal, 60(6), 5579-5590.

Ferrer-González, E., Aguera-Vega, F., Carvajal-Ramirez, F., & Martínez-Carricondo, P. (2020). UAV photogrammetry accuracy assessment for corridor mapping based on the number and distribution of ground control points. Remote Sensing, 12(15), 2447. Available at: https://www.mdpi.com/2072-4292/12/15/2447.

Galo, M., & Camargo, P. de O. (1994). Utilização do GPS no controle de qualidade de cartas. In Congresso Brasileiro de Cadastro Técnico Multifinalitário (pp. 41-48).

Hardin, P. J., & Jensen, R. R. (2011). Small-scale unmanned aerial vehicles in environmental remote sensing: Challenges and opportunities. GIScience & Remote Sensing, 48(1), 99-111.

James, M. R., Robson, S., d'Oleire-Oltmanns, S., & Niethammer, U. (2017). Optimising UAV topographic surveys processed with structure-from-motion: Ground control quality, quantity, and bundle adjustment. Geomorphology, 280, 51-66.

Javernick, L., Brasington, J., & Caruso, B. (2014). Modeling the topography of shallow braided rivers using structure-from-motion photogrammetry. Geomorphology, 213, 166-182.

Kraus, K. (2011). Photogrammetry: Geometry from images and laser scans (2nd ed.). Berlin, Germany: de Gruyter.

Meinen, B. U., & Robinson, D. T. (2020). Streambank topography: An accuracy assessment of UAV-based and traditional 3D reconstructions. International Journal of Remote Sensing, 41(1), 1-18.

Rehak, M., & Skaloud, J. (2015). Fixed-wing micro aerial vehicle for accurate corridor mapping. ISPRS Annals of Photogrammetry, Remote Sensing & Spatial Information Sciences, 2.

Sopchaki, C. H., da Paz, O. L. de S., Graça, N. L. S. de S., & Sampaio, T. V. M. (2018). Verificação da qualidade de ortomosaicos produzidos a partir de imagens obtidas com aeronave remotamente pilotada sem o uso de pontos de apoio. Raega - O Espaço Geográfico em Análise, 43, 200-214.

Szeliski, R. (2010). Computer vision: Algorithms and applications. Springer Science & Business Media.

Westoby, M. J., Brasington, J., Glasser, N. F., Hambrey, M. J., & Reynolds, J. M. (2012). 'Structure-from-motion' photogrammetry: A low-cost, effective tool for geoscience applications. Geomorphology, 179, 300-314.